2-2018

Fault Mode Probability Factor Based Fault-Tolerant Control for Dissimilar Redundant Actuation System

Jun Wang

Shaoping Wang

Xingjian Wang

Mileta M. Tomovic
Old Dominion University, mtomovic@odu.edu

Cun Shi

Original Publication Citation

Wang, J., Wang, S. P., Wang, X. J., Tomovic, M. M., & Shi, C. (2018). Fault mode probability factor based fault-tolerant control for dissimilar redundant actuation system. *Chinese Journal of Aeronautics, 31*(5), 965-975. doi:10.1016/j.cja.2018.01.026

Chinese Journal of Aeronautics, (2018), 31(5): 965–975

Chinese Society of Aeronautics and Astronautics
& Beihang University

Chinese Journal of Aeronautics

cja@buaa.edu.cn
www.sciencedirect.com

Fault mode probability factor based fault-tolerant control for dissimilar redundant actuation system

Jun WANG [a], Shaoping WANG [a], Xingjian WANG [a,*], Mileta M. TOMOVIC [b], Cun SHI [a]

[a] *School of Automation Science and Electrical Engineering, Beihang University, Beijing 100083, China*
[b] *College of Engineering and Technology, Old Dominion University, Norfolk, VA 23529, USA*

Received 7 March 2017; revised 17 August 2017; accepted 20 November 2017
Available online 15 February 2018

KEYWORDS

Dissimilar redundant actuation system;
Fault mode probability factor;
Fault-tolerant control;
Linear quadratic regulator;
Monte Carlo simulation;
Moving window

Abstract This paper presents a Fault Mode Probability Factor (FMPF) based Fault-Tolerant Control (FTC) strategy for multiple faults of Dissimilar Redundant Actuation System (DRAS) composed of Hydraulic Actuator (HA) and Electro-Hydrostatic Actuator (EHA). The long-term service and severe working conditions can result in multiple gradual faults which can ultimately degrade the system performance, resulting in the system model drift into the fault state characterized with parameter uncertainty. The paper proposes to address this problem by using the historical statistics of the multiple gradual faults and the proposed FMPF to amend the system model with parameter uncertainty. To balance the system model precision and computation time, a Moving Window (MW) method is used to determine the applied historical statistics. The FMPF based FTC strategy is developed for the amended system model where the system estimation and Linear Quadratic Regulator (LQR) are updated at the end of system sampling period. The simulations of DRAS system subjected to multiple faults have been performed and the results indicate the effectiveness of the proposed approach.

1. Introduction

Dissimilar Redundant Actuation Systems (DRAS), composed of Hydraulic Actuator (HA) and Electro-Hydrostatic Actuator (EHA), have been increasingly gaining consideration for the application in the large commercial aircraft due to their ability to avoid possible common mode failures.[1–3] DRAS has the advantage of fast response and high reliability associated with HA actuator, while avoiding common mode failure by introducing redundant EHA.[4] The research on DRAS system has become the mainstream of the large aircraft development programs. The latest Airbus aircraft, A380 and A350, have adopted DRAS system of 2H/2E type.[5]

The HA systems commonly experience gradual faults caused by oil leakage and constriction of oil flow which ultimately lead to the system performance degradation. Although

* Corresponding author.
E-mail address: wangxj@buaa.edu.cn (X. WANG).
Peer review under responsibility of Editorial Committee of CJA.

ELSEVIER Production and hosting by Elsevier

https://doi.org/10.1016/j.cja.2018.01.026
1000-9361

these faults may have limited initial side-effect, over the long life-time they can result in increasingly adverse effects on the actuation system and impact the overall system performance. Therefore, measures must be taken to maintain certain level of acceptable system performance under the gradually increasing system fault conditions. The Fault-Tolerant Control (FTC) techniques[6–8] are commonly used to remedy the faults and maintain the aircraft system safety at a high level, and could also be applied to designing the FTC mechanism for the actuation system with gradual faults.

Design of FTC system requires that the system parameters be known, which is difficult to realize in real application.[9] Researchers have proposed various control methods for uncertain systems operating under very specific working conditions and for short period of time, specifically, for the cases when gradual faults do not have significant effect on the system performance. However, there are few control methods for systems with varying and uncertain parameters over long period of time, which prompted many researchers to focus on the system identification techniques[10–13] commonly applied to systems under normal operating conditions and over a specific time period. However, when system faults occur, the corresponding system parameters would drift, which would increase the identification errors of the parameter values. When the system suffers multiple faults of different severity levels, the system parameters would present uncertainty. Therefore, traditional approaches addressing system identification are inadequate for effective control design for the systems with increasing errors of parameters. This is especially evident in the case of a system with changing parameters caused by the gradual faults of the imprecise system model. The robust control techniques,[14,15] adaptive design techniques[16,17] and the Linear Parameter Varying (LPV) control design methods[18] can deal with the system uncertainty to some degree, but they exhibit limitations when applied to systems with multiple gradual faults which occur over a long working period.

Design of an effective FTC mechanism for DRAS experiencing gradual faults, is a complex problem which involves not only system identification over a long period of time but also design of the fault-tolerant controller. This paper proposes a Fault Mode Probability Factor (FMPF) based FTC strategy for multiple fault modes of DRAS over a long working period. Since the identification errors would increase due to the multiple gradual faults, the cycle of sampling method is used to record the multiple fault modes and provide the historical statistics as the fault information. Applying the proposed FMPF with expectation operator, the historical statistics can be used to estimate current degree and values of multiple faults. Finally, the amended system model based on FMPF can be obtained and used to design the fault-tolerant controller. Based on the amended system model, the control gain can be determined using Linear Quadratic Regulator (LQR).[19–21] To balance the system model precision and the computation time, a Moving Window (MW) method is used to determine the amount of applied historical statistics, following a certain window size, at the end of the most recent sampling period, new system parameter estimation results are imported into the applied historical statistics while the oldest set is removed, and then the chosen historical statistics are processed by using the FMPF to update the system parameters. The updated system parameters are then used to modify the control law to compensate for the effects of the changed gradual faults. In this paper, the Monte Carlo method is used to provide simulation data for different periods. Several case studies of DRAS, subjected to multiple faults, are performed to analyze the effectiveness of this method and associated design approach.

The main contribution of this paper is the FMPF based FTC strategy for multiple fault modes of DRAS under long term working conditions, where the control gain of the fault-tolerant controller is updated with each sampled data set. This approach allows the system performance to be maintained within reasonable range even under changed working conditions caused by the gradual faults. Compared with the existing FTC design methods, the proposed FMPF approach applies the expectation operator on the historical statistics resulting in a novel way to comprehensively utilize the system statistical information, where law of large numbers and central limit theorem can be used to provide theoretical foundations, and meanwhile, the MW method balances the system model precision and the computation time.

Notation: Throughout this paper, the superscript T specifies matrix transposition, Δ specifies parameter error. The symbol P stands for probability and E expectation operator. $\mathrm{Re}\{\boldsymbol{\lambda}(\cdot)\}$ is the form of eigenvalue real part. $w(t) \in L_2[0, \infty)$ is a quadratic differential function. $\max(\cdot)$ and $\min(\cdot)$ express maximum value and minimum value respectively.

2. System description

The DRAS system is composed of one HA system and one EHA system as shown in Fig. 1. In the normal operating condition, only HA drives the control surface while EHA is in the follower mode, i.e. backup mode. This type of active/passive (A/P) operating mode, known as H_A/E_P mode, is the most common operating mode since HA system has better performance than EHA system. Consequently, the proposed FTC strategy is developed for this operating mode and leaves the E_A/H_P operating mode as an alternate FTC strategy.

2.1. Modeling of H_A/E_P mode under normal operating condition

The model of H_A/E_P system, used in this work, has been previously developed and published by this research group.[22] The model is based on the assumption that the control surface is a rigid body of known mass and inertial moments. The forces acting on the system include the HA cylinder force, F_h, inertial and damping load of the EHA system, and aerodynamic force, F_L. The state space representation of the system is given as follows:

$$\begin{cases} \dot{\boldsymbol{x}}(t) = \boldsymbol{A}\boldsymbol{x}(t) + \boldsymbol{B}\boldsymbol{u}(t) + \boldsymbol{G}\boldsymbol{w}(t) \\ \boldsymbol{y}(t) = \boldsymbol{C}\boldsymbol{x}(t) \end{cases} \tag{1}$$

where the state vector is defined as $\boldsymbol{x}(t) = [x_h, \dot{x}_h, P_h, x_v]^T$, x_h and $\dot{x}_h$ are the velocity and acceleration of the piston respectively, P_h is the cylinder pressure, and x_v is the servo valve displacement; $\boldsymbol{u}(t)$ is the system input to be designed; $\boldsymbol{y}(t)$ is the system output; $\boldsymbol{w}(t)$ is unknown disturbance. The state, input, output, and disturbance matrices are as follows[23]:

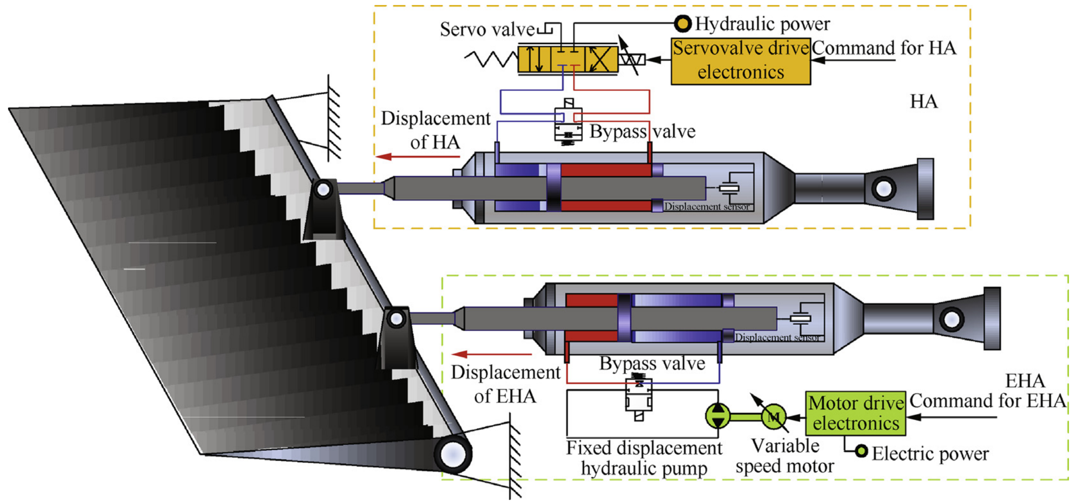

Fig. 1 Schematic of dual DRAS system.

$$\begin{cases} \boldsymbol{A} = \begin{bmatrix} 0 & 1 & 0 & 0 \\ 0 & -\frac{B_h+B_e+B_d}{m_h+m_e+m_d} & \frac{A_h}{m_h+m_e+m_d} & 0 \\ 0 & -\frac{4E_hA_h}{V_h} & -\frac{4E_hK_{ce}}{V_h} & \frac{4E_hK_q}{V_h} \\ 0 & 0 & 0 & -\frac{1}{\tau_v} \end{bmatrix} \\ \boldsymbol{B} = \left[0, 0, 0, \frac{K_v}{\tau_v}\right]^T \\ \boldsymbol{C} = \begin{bmatrix} 1 & 0 & 0 & 0 \\ 0 & 1 & 0 & 0 \\ 0 & 0 & 1 & 0 \\ 0 & 0 & 0 & 1 \end{bmatrix} \\ \boldsymbol{G} = \left[0, -\frac{1}{m_h+m_e+m_d}, 0, 0\right]^T \end{cases} \tag{2}$$

where B_h, B_e and B_d are damping coefficients of hydraulic cylinders of HA and EHA systems, and the control surface; m_h, m_e and m_d are masses of hydraulic cylinder pistons of HA and EHA systems and the control surface; A_h is hydraulic cylinder area of HA; V_h is the hydraulic cylinder total volume of HA; E_h is bulk modulus; $K_{ce} = (K_c + C_{hl})$, K_c is coefficient of flow-pressure, and C_{hl} is leakage coefficient of hydraulic cylinder of HA; K_q is coefficient of flow change; K_v is proportionality coefficient of servo valve; τ_v is the servo valve time constant.

2.2. Modeling of H_A/E_P mode with multiple gradual faults

According to the published research,[24,25] the gradual faults of HA, which cause the parameters drift, can be classified in the following five types: (A) the change of servo valve time constant τ_v due to the servo valve blockage; (B) the change of servo valve gain K_v due to the servo valve leakage; (C) the change of bulk modulus E_h due to the air entrapment in oil; (D) the change of damping coefficient B_h due to the increasing motion damping; (E) the change of leakage coefficient C_{hl} due to the hydraulic cylinder leakage. These types of gradual faults may be difficult to detect but would result in degradation of the system performance. The uncertainty modulation matrices are used to model these faults in DRAS system and to describe the parameter uncertainty caused by these faults. Assuming that the system does not experience sensor faults, the DRAS model of the H_A/E_P mode with gradual faults can be represented in the following form:

$$\begin{cases} \dot{\boldsymbol{x}}(t) = (\boldsymbol{A} + \Delta\boldsymbol{A})\boldsymbol{x}(t) + (\boldsymbol{B} + \Delta\boldsymbol{B})\boldsymbol{u}(t) + \boldsymbol{Gw}(t) \\ \boldsymbol{y}(t) = \boldsymbol{Cx}(t) \end{cases} \tag{3}$$

where $\Delta\boldsymbol{A}$ and $\Delta\boldsymbol{B}$ are deviations in the original state and input matrices caused by parameter change due to the system faults. The system matrices and the fault modulation matrices can be expressed as follows:

$$\begin{cases} \boldsymbol{A} = \begin{bmatrix} 0 & 1 & 0 & 0 \\ 0 & a_{22} & a_{23} & 0 \\ 0 & a_{32} & a_{33} & a_{34} \\ 0 & 0 & 0 & a_{44} \end{bmatrix} \\ \boldsymbol{B} = [0, 0, 0, b_4]^T \\ \Delta\boldsymbol{A} = \begin{bmatrix} 0 & 1 & 0 & 0 \\ 0 & \Delta a_{22} & \Delta a_{23} & 0 \\ 0 & \Delta a_{32} & \Delta a_{33} & \Delta a_{34} \\ 0 & 0 & 0 & \Delta a_{44} \end{bmatrix} \\ \Delta\boldsymbol{B} = [0, 0, 0, \Delta b_4]^T \end{cases} \tag{4}$$

where coefficients $\boldsymbol{A}$ and $\boldsymbol{B}$ matrices are defined in Eq. (2), whereas $\Delta a_{22} = -\Delta B_h/(m_h + m_e + m_d)$ is damping fault factor, $\Delta a_{32} = -4\Delta E_h A_h/V_h$ is the bulk modulus fault factor, $\Delta a_{33} = -[4\Delta E_h(K_c + \Delta C_{hl})]/V_h$ represents the bulk modulus and the internal leakage fault factor, $\Delta a_{34} = 4\Delta E_h K_q/V_h$ represents the bulk modulus fault factor, $\Delta a_{44} = -1/\Delta\tau_v$ is the servo valve time constant fault factor, and $\Delta b_{41} = \Delta K_v/\Delta\tau_v$ represents the servo valve block and leakage failure factor.

3. Amended model based on fault mode probability factor

Since gradual faults have stochastic characteristics, they can be described using probabilistic approach. As the gradual faults converge to a particular state, that state can be regarded as the expectation of the final gradual fault changed state and could be used to describe the gradual fault process and design appropriate FTC strategy.

The effects of all the gradual faults have been modeled as uncertainty matrices $\Delta\boldsymbol{A}$ and $\Delta\boldsymbol{B}$ which can be regarded as random variables $(\Delta\boldsymbol{A}(t), \Delta\boldsymbol{B}(t))$ due to the gradual change of DRAS faults. The matrices $(\Delta\boldsymbol{A}_{T_i}, \Delta\boldsymbol{B}_{T_i})$ are updated after every sampling period T followed by the parameter estimation procedure, where T_i is the ith sampling period. According to Law of Large Numbers and the gradual change of DRAS faults, the matrix class sequence of gradual fault parameters will converge to the expected value $(\Delta\boldsymbol{A}_{\mathrm{E}}, \Delta\boldsymbol{B}_{\mathrm{E}})$,

$$P\left(\lim_{T_i\to\infty}(\Delta\boldsymbol{A}_{T_i}, \Delta\boldsymbol{B}_{T_i}) = (\Delta\boldsymbol{A}_{\mathrm{E}}, \Delta\boldsymbol{B}_{\mathrm{E}})\right) = 1 \tag{5}$$

Since the matrix class sequence $(\Delta\boldsymbol{A}_{T_i}, \Delta\boldsymbol{B}_{T_i})$ can be obtained from periodically sampled historical statistics, and since they may vary only with the sampling period, therefore, if there are N sets of the sequence $(\Delta\boldsymbol{A}_{T_1}, \Delta\boldsymbol{B}_{T_1}) \to (\Delta\boldsymbol{A}_{T_N}, \Delta\boldsymbol{B}_{T_N})$, they can be regarded as independent with the same distribution. Since the matrix class sequence is historical statistics of gradual faults at different periods, the sequence can have limited non-zero matrix variance σ^2. Therefore, according to the central limit theorem, the error with the expectation $(\Delta\boldsymbol{A}_{\mathrm{E}}, \Delta\boldsymbol{B}_{\mathrm{E}})$ can be described as

$$\lim_{N\to\infty} P\left(\frac{\sqrt{N}}{\sigma}\left|(\Delta\boldsymbol{A}_{T_N}, \Delta\boldsymbol{B}_{T_N}) - (\Delta\boldsymbol{A}_{\mathrm{E}}, \Delta\boldsymbol{B}_{\mathrm{E}})\right| < (\delta\boldsymbol{A}, \delta\boldsymbol{B})\right) = \frac{1}{\sqrt{2\pi}}\int_{-(\delta\boldsymbol{A},\delta\boldsymbol{B})}^{(\delta\boldsymbol{A},\delta\boldsymbol{B})} \mathrm{e}^{-t^2/2}\mathrm{d}t \tag{6}$$

If there is sufficient amount of historical statistics, namely, for sufficiently large sampling number N, the error distribution can be described as

$$P\left(\frac{\sqrt{N}}{\sigma}\left|(\Delta\boldsymbol{A}_{T_N}, \Delta\boldsymbol{B}_{T_N}) - (\Delta\boldsymbol{A}_{\mathrm{E}}, \Delta\boldsymbol{B}_{\mathrm{E}})\right| < (\delta\boldsymbol{A}, \delta\boldsymbol{B})\right) \approx \frac{1}{\sqrt{2\pi}}\int_{0}^{(\delta\boldsymbol{A},\delta\boldsymbol{B})} \mathrm{e}^{-t^2/2}\mathrm{d}t = 1-\alpha \tag{7}$$

where α is the confidence coefficient. This approach provides a way to modify the system model under gradual fault conditions, which is affected by the number of the historical sampling sets.

3.1. Moving window based determination principle for historical statistics

Eq. (6) shows that as historical statistics set number N becomes larger, the probability of the error between the matrix class sequence and their expectation will be close to the normal distribution, namely, increasing historical statistics will result in increased accuracy of expectation. However, two factors need to be considered: (A) although a large number of applied historical statistics within reasonable time range can be used to estimate a more accurate set of system parameters, they also increase the computation time, and (B) very old historical statistics can have negative effect when used to estimate the current system parameters. To balance the system model precision with required computation time, a MW method is introduced to reduce the negative effect of the old historical statistics.

The principle of the moving window is shown in Fig. 2. Considering both of the previously mentioned factors and assuming that the optimal MW size is $S_{\mathrm{MW}} = (N-1)T$, the MW is changing from MW(1) to MW$(N-1)$ (marked in green) before the MW reaches its desired length. During this period, increasing amount of historical statistics is used, and once the MW size achieves its optimal length $(N-1)T$, it will continue to maintain that length (marked in red). In the process, the old historical statistics will be removed from the applied set while the new statistics will be applied. Using the MW with its size of $(N-1)T$, there are always N set of historical statistics used to estimate the system model parameters.

Remark 1. In Eq. (7), the confidence coefficient α is defined to measure the estimation accuracy of the system model parameters. Given a defined acceptable maximum value $\alpha_{\max}$, the determined optimal MW size S_{MW} should guarantee that $\alpha \leqslant \alpha_{\max}$ holds. Considering the computation time by defining the computation time cost as $t(\mathrm{cost})$, the S_{MW} should guarantee that $t(\mathrm{cost}) \leqslant t_{\max}$. Therefore, MW size can be regarded as a multivariate function $S_{\mathrm{MW}} = F(\{\alpha|\alpha \leqslant \alpha_{\max}\}, \{t(\mathrm{cost})|t(\mathrm{cost}) \leqslant t_{\max}\})$, which can be used to determine the optimal MW size $S_{\mathrm{MW}}^{\mathrm{optimal}}$ by an optimization process.

3.2. Fault mode probability factor

In order to effectively utilize the historical statistics of the fault modes, the FMPF is proposed in this paper. The multiple faults occur at different levels and in different combinations, which can cause residual statistical information for the multiple faults. Choosing reasonable sampling period over the long working period, the gradual fault parameter change can be saved as historical statistics. The multiple faults can be represented by the parameter-dependent matrices of the state space form system as $(\Delta\boldsymbol{A}_{T_i}, \Delta\boldsymbol{B}_{T_i})$. In all historical statistics, different matrix classes may be the same, namely, in different sampling periods: $(\Delta\boldsymbol{A}_{T_i}, \Delta\boldsymbol{B}_{T_i}) = (\Delta\boldsymbol{A}_{T_j}, \Delta\boldsymbol{B}_{T_j})$. In order to appropriately apply the historical statistics to design the FTC law, the FMPF method is first defined as follows:

Definition 1. FMPF. The probability of the multiple faults represents a combination of different faults at different degrees of fault severity, which is captured through statistical information. If there are N cycles of historical statistics, and some of the historical statistics are the same, the same historical statistics are captured in the same group and recorded with the number n_{c_j}, where c_j is the jth category of the historical statistics. Define the fault mode probability factor as

$$P_{c_j} = n_{c_j}/N \tag{8}$$

where n_{c_j} can be used to describe the probability of the jth category of multiple faults $(\Delta\boldsymbol{A}_{T_i}, \Delta\boldsymbol{B}_{T_i})_{c_j}$. In addition, if there are total of k multiple categories of the historical statistics, all the FMPFs can be calculated as $\{P_{c_1}, P_{c_2}, \cdots, P_{c_k}\}$. From all the calculated FMPFs, let $P_{\max} = \max\{P_{c_1}, P_{c_2}, \cdots, P_{c_k}\}$ be the maximum probability factor, where in the case of $P_{c_j} = P_{\max}$, the jth category multiple faults $(\Delta\boldsymbol{A}_{T_i}, \Delta\boldsymbol{B}_{T_i})_{c_j}$ is the most common fault condition during the entire measured statistical time interval.

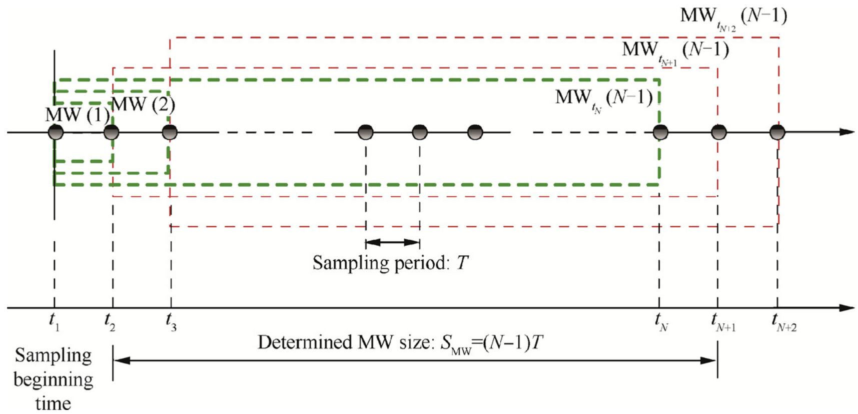

Fig. 2 Moving window based applied historical statistics determination mechanism.

Since the current system with multiple faults in uncertain form can be amended using the historical statistics, the amended model based on FMPF is given in the following section.

3.3. Amended model based on fault mode probability factor

The proposed approach to deal with the system uncertainty is amending the uncertain system in state space form using FMPF. As a result, the uncertain matrices $(\Delta\boldsymbol{A},\Delta\boldsymbol{B})$, which describe the multiple faults in the system, can be determined using FMPF and the corresponding historical statistics. Since all gradual faults converge to a specific state, the expectation operator, Eq. (5), can be applied to processing the statistics and amending the system model uncertainty as $(\Delta\boldsymbol{A}_{\mathrm{E}},\Delta\boldsymbol{B}_{\mathrm{E}})=\lim_{t\to\infty}E(\Delta\boldsymbol{A},\Delta\boldsymbol{B})$. Specifically, the expectation operator based on FMPF can be used in the following form:

$$(\Delta\boldsymbol{A}_{\mathrm{E}},\Delta\boldsymbol{B}_{\mathrm{E}})=\left(\sum_{j=1}^{k}(P_{c_j}(\Delta\boldsymbol{A}_{T_i})),\sum_{j=1}^{k}(P_{c_j}(\Delta\boldsymbol{B}_{T_i}))\right) \tag{9}$$

where k is the number of the multiple fault mode categories. The proposed FMPF of the historical statistics and the expectation operator can be used to amend DRAS system with multiple faults as

$$\begin{cases}\dot{\boldsymbol{x}}(t)=\left[\boldsymbol{A}+\left(\sum_{j=1}^{k}(P_{c_j}(\Delta\boldsymbol{A}_{T_i}))\right)\right]\boldsymbol{x}(t)\\ \qquad+\left[\boldsymbol{B}+\left(\sum_{j=1}^{k}(P_{c_j}(\Delta\boldsymbol{B}_{T_i}))\right)\right]\boldsymbol{u}(t)+\boldsymbol{G}\boldsymbol{w}(t)\\ \boldsymbol{y}(t)=\boldsymbol{C}\boldsymbol{x}(t)\end{cases} \tag{10}$$

In this amended model, the system uncertain matrices $(\Delta\boldsymbol{A},\Delta\boldsymbol{B})$ can be replaced by the determinant expectation of matrices $(\sum_{j=1}^{k}(P_{c_j}(\Delta\boldsymbol{A}_{T_i})),\sum_{j=1}^{k}(P_{c_j}(\Delta\boldsymbol{B}_{T_i})))$ based on FMPF. Finally, the amended system model can be described as

$$\begin{cases}\dot{\boldsymbol{x}}(t)=(\boldsymbol{A}+\Delta\boldsymbol{A}_{\mathrm{E}})\boldsymbol{x}(t)+(\boldsymbol{B}+\Delta\boldsymbol{B}_{\mathrm{E}})\boldsymbol{u}(t)+\boldsymbol{G}\boldsymbol{w}(t)\\ \boldsymbol{y}(t)=\boldsymbol{C}\boldsymbol{x}(t)\end{cases} \tag{11}$$

The purpose of the FMPF based approach is to counteract the adverse effect of parameter uncertainty since it can reduce the parameter estimation errors by utilizing the historical statistics and expectation operator, and then to facilitate the FTC strategy design based on the amended system model. The theoretical foundation of the FMPF based approach is illustrated by the following lemma.

Lemma 1. The FMPF based amended model is more accurate than the uncertain model under the condition of the multiple gradual faults. Namely, using the same feedback matrix, the absolute values of the error between the real parts of eigenvalues for the FMPF based amended model and the actual one, and the error between the real parts of eigenvalues for the uncertain model and the actual one, hold up Eq. (A11).

Proof. See Appendix A.

Based on the amended model in Eq. (11), the controller of the FTC strategy is designed in the following section.

4. Design of FMPF based FTC strategy

The flowchart of FMPF based FTC approach is presented in Fig. 3. In the initial stage of the actuation system, whether the gradual faults occur or not, a set of baseline control parameters should be determined. Since the gradual faults are being considered, all the relevant parameters of gradual faults should be preset and used to construct the uncertain matrices of the system model. Reasonable thresholds of parameters due to gradual faults within the FTC range are chosen. The gradual faults occur during a very long term, and in order to determine reasonable control parameters under gradual faults condition, a control parameter updating period is chosen. At every end of the period, the relevant parameters of gradual faults are estimated using system identification techniques. If all the parameters are within the corresponding thresholds, these parameters are then saved as a new set of the historical statistics. However, if some of the parameters deviate sharply from the corresponding thresholds, it can be conjectured that severe faults have occurred and that the current FTC law should be switched to another one.[23] In the case when the parameters move slightly outside the corresponding thresholds, the relevant control parameter matrices need to be appropriately adjusted. When the new set of gradual fault parameters is added to the historical statistics, the FMPF needs to be updated and the expectation parameter matrices of gradual faults need to be determined based on the new FMPF. Since the obtained system model, under gradual fault conditions, is determined

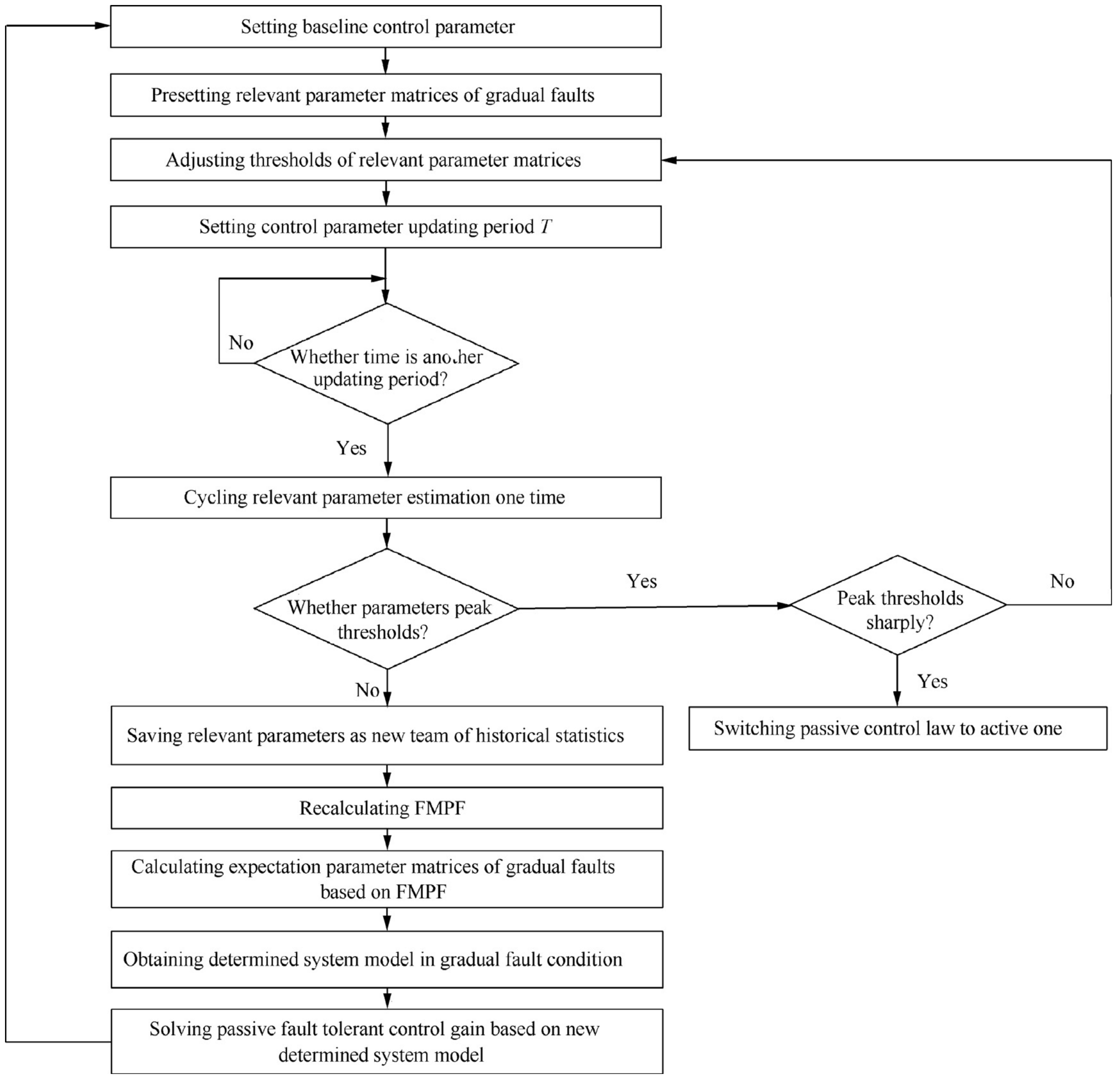

Fig. 3 Flowchart of FMPF based FTC mechanism.

by replacing the uncertain matrices with the expectation parameter matrices, the new FTC gain based on new determined system model can be solved and used to update the previous one.

The particular form of FTC for DRAS system with multiple gradual faults is introduced in the following sections.

It is assumed that the controller has fixed structure[26,27] such that:

(1) Under the multiple gradual faults condition, DRAS output can track the command order $\boldsymbol{S}_{\text{out}}\boldsymbol{y}(t)$ with respect to the reference signal $\boldsymbol{r}(t)$ without steady-state error, i.e. $\lim_{t\to\infty}\boldsymbol{e}(t)=\boldsymbol{0}$, where $\boldsymbol{e}(t)=\boldsymbol{r}(t)-\boldsymbol{S}_{\text{out}}\boldsymbol{y}(t)$, and $\boldsymbol{S}_{\text{out}}=[1,0,0,0]$.

(2) The optimized performance defined in Eq. (14) can be obtained through the designed controller. The corresponding augmented system can be described in the following form:

$$\begin{cases}\dot{\boldsymbol{x}}_{\text{aug}}(t)=\boldsymbol{A}_{\text{aug}}\boldsymbol{x}_{\text{aug}}(t)+\boldsymbol{B}_{\text{aug}}\boldsymbol{u}(t)+\boldsymbol{G}_{\text{aug}}\boldsymbol{w}_{\text{aug}}(t)\\ \boldsymbol{y}_{\text{aug}}(t)=\boldsymbol{C}_{\text{aug}}\boldsymbol{x}_{\text{aug}}(t)\end{cases} \tag{12}$$

where $\boldsymbol{x}_{\text{aug}}(t)=[\int\boldsymbol{e}(t)\text{d}t,\boldsymbol{x}(t)]^{\text{T}}$ is augmented state vector, $\boldsymbol{y}_{\text{aug}}(t)=[\int\boldsymbol{e}(t)\text{d}t,\boldsymbol{y}(t)]^{\text{T}}$ is augmented output vector, and $\boldsymbol{w}_{\text{aug}}(t)=[\boldsymbol{r}(t),\boldsymbol{w}(t)]^{\text{T}}$ is augmented disturbance vector. The corresponding augmented matrices are $\boldsymbol{A}_{\text{aug}}=\begin{bmatrix}\boldsymbol{0} & -\boldsymbol{S}_{\text{out}}\boldsymbol{C}\\ \boldsymbol{0} & \boldsymbol{A}+\boldsymbol{A}_{\text{E}}\end{bmatrix}$, $\boldsymbol{B}_{\text{aug}}=\begin{bmatrix}\boldsymbol{0}\\ \boldsymbol{B}+\boldsymbol{B}_{\text{E}}\end{bmatrix}$, $\boldsymbol{C}_{\text{aug}}=\begin{bmatrix}\boldsymbol{I} & \boldsymbol{0}\\ \boldsymbol{0} & \boldsymbol{C}\end{bmatrix}$, and $\boldsymbol{G}_{\text{aug}}=\begin{bmatrix}\boldsymbol{I} & \boldsymbol{0}\\ \boldsymbol{0} & \boldsymbol{G}\end{bmatrix}$. The controllability of this augmented system can be determined from its controllability verification matrix $\boldsymbol{C}_{\text{con}}=[\boldsymbol{B}_{\text{aug}},\boldsymbol{A}_{\text{aug}}\boldsymbol{B}_{\text{aug}},\boldsymbol{A}_{\text{aug}}^2\boldsymbol{B}_{\text{aug}},\boldsymbol{A}_{\text{aug}}^3\boldsymbol{B}_{\text{aug}},\boldsymbol{A}_{\text{aug}}^4\boldsymbol{B}_{\text{aug}}]$.

In order to guarantee that the output can track the input signal, the controller is designed as per Ref. [28] by using the state and output error integration feedback as follows:

$$\boldsymbol{u}(t)=\boldsymbol{K}\boldsymbol{x}_{\text{aug}}(t)=\boldsymbol{K}_e\int_0^t e(\tau)\text{d}\tau+\boldsymbol{K}_x\boldsymbol{x}(t) \tag{13}$$

where $\boldsymbol{K}=[\boldsymbol{K}_e,\boldsymbol{K}_x]$ is the control gain matrix. The poles of this augmented system can be selected to have negative real parts, thus guaranteeing stability of the closed-loop system.

The Linear-Quadratic (LQ) cost function is defined in the following form:

$$J = \int_0^t (\boldsymbol{x}_{\mathrm{aug}}^{\mathrm{T}}(\tau)\boldsymbol{Q}\boldsymbol{x}_{\mathrm{aug}}(\tau) + \boldsymbol{u}(\tau)^{\mathrm{T}}\boldsymbol{R}\boldsymbol{u}(\tau))\mathrm{d}\tau \tag{14}$$

where $\boldsymbol{Q}$ and $\boldsymbol{R}$ are symmetric semi-positive-definite and positive-definite weighting matrices, respectively. The control law can be obtained by selecting the state weighting matrix $\boldsymbol{Q}$ and input weighting matrix $\boldsymbol{R}$, so as to minimize the total control cost function $\boldsymbol{J}$. The optimal solution to minimize the total control cost can be obtained by solving the following Riccati equation:

$$\boldsymbol{P}\boldsymbol{A}_{\mathrm{aug}} + \boldsymbol{A}_{\mathrm{aug}}^{\mathrm{T}}\boldsymbol{P} - \boldsymbol{P}\boldsymbol{B}_{\mathrm{aug}}\boldsymbol{R}^{-1}\boldsymbol{B}_{\mathrm{aug}}^{\mathrm{T}}\boldsymbol{P} + \boldsymbol{Q} = \boldsymbol{0} \tag{15}$$

where $\boldsymbol{P}$ is a positive-definite matrix. The feedback control gain matrix $\boldsymbol{K} = [\boldsymbol{K}_e, \boldsymbol{K}_x]$ can be determined by using LQR,

$$[\boldsymbol{K}_e, \boldsymbol{K}_x] = -\boldsymbol{R}^{-1}\boldsymbol{B}_{\mathrm{aug}}^{\mathrm{T}}\boldsymbol{P} \tag{16}$$

Remark 2. The parameter γ represents the robust performance of the system and describes the quantitative relationship between the disturbance $\boldsymbol{w}$ and the system output $\boldsymbol{y}$. The inequality $\|\boldsymbol{G}(\boldsymbol{s})\| < \gamma$ means that the influence of the disturbance $\boldsymbol{w}$ on the system output $\boldsymbol{y}$ is limited in the gain level γ.

The controller with FTC function (Fig. 4) is in the state and output error integration feedback form to realize the pole placement and guarantee desired performance in the presence of disturbance. The system uncertainty, due to multiple faults, is addressed by applying the matrix class sequence $(\Delta\boldsymbol{A}_{T_i}, \Delta\boldsymbol{B}_{T_i})$ to obtain the matrices $(\sum_{j=1}^{k}(P_{c_j}(\Delta\boldsymbol{A}_{T_i})), \sum_{j=1}^{k}(P_{c_j}(\Delta\boldsymbol{B}_{T_i})))$ using the proposed FMPF method. To minimize the cost function, Eq. (14), the weighting matrices can be chosen from LQR, and then the control gain matrix for the uncertain system can be solved. The condition for finding the fault-tolerant controller gain is given by the following theorem.

Theorem 1. Considering the closed-loop augmented system given by Eq. (12), for a given scalar $\gamma > 0$ in Remark 1 and for all nonzero disturbances$w(t) \in L_2[0, \infty)$, choosing $\boldsymbol{Q}$ and $\boldsymbol{R}$ as weighting matrices of LQ index, and defining symmetric positive definite matrix $\boldsymbol{P}$, if the LQR can find the $\boldsymbol{P}$ matrix, then the closed-loop system given in Eq. (12) has the upper bounds of performance index given in the following form:

$$J < \boldsymbol{x}_{\mathrm{aug}}^{\mathrm{T}}(0)\boldsymbol{P}\boldsymbol{x}_{\mathrm{aug}}(0) + \gamma^2\int_0^t \boldsymbol{w}_{\mathrm{aug}}^{\mathrm{T}}(\tau)\boldsymbol{w}_{\mathrm{aug}}(\tau)\mathrm{d}\tau \tag{17}$$

and the gain matrix for the fault-tolerant controller of the closed-loop system can be determined as $[\boldsymbol{K}_e, \boldsymbol{K}_x] = -\boldsymbol{R}^{-1}\boldsymbol{B}_{\mathrm{aug}}^{\mathrm{T}}\boldsymbol{P}$.

Proof. See Appendix B.

5. Simulation analysis

5.1. Settings of fault scenarios

The system parameters used to verify the effectiveness of the proposed approach are the same as those used in Ref.[22] Typical multiple gradual faults of HA system are presented in Section 2.2. In order to demonstrate the advantage of the proposed FMPF based FTC approach, the Monte Carlo simulation method is used to simulate the historical statistics. Assuming that the MW size is $S_{\mathrm{MW}} = 30$ and that it can satisfy the computation time cost requirement, the historical statistics are then processed using FMPF method and the expectation operator to obtain five different amended model results, which are designated as FMPF-1 to FMPF-5 and are shown in Table 1.

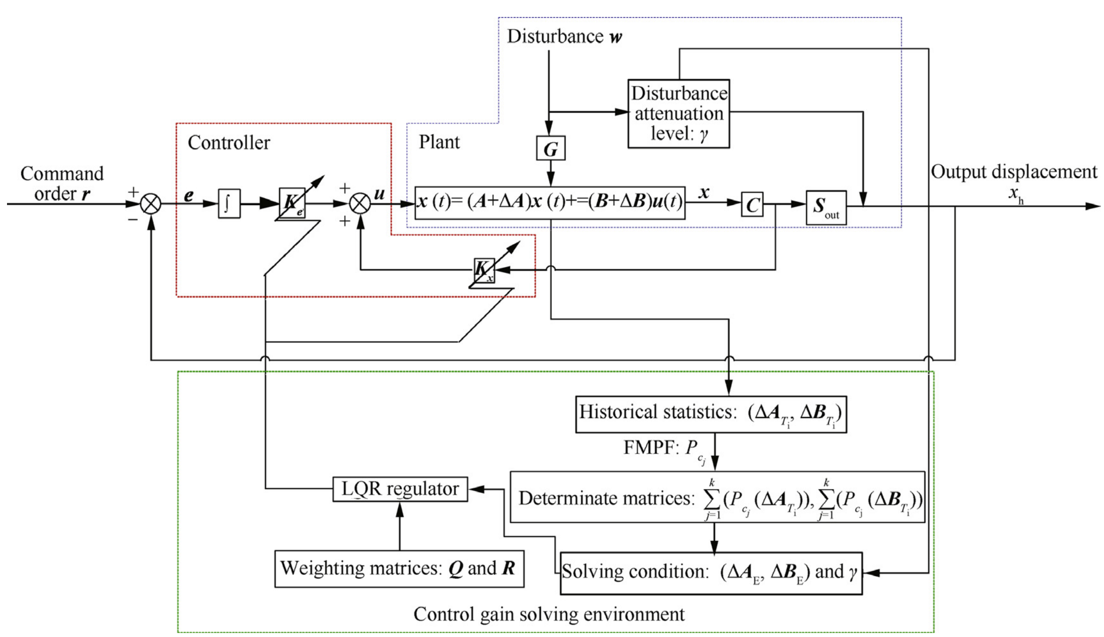

Fig. 4 Controller structure for system with multiple faults in uncertainty form.

Table 1 Historical statistics of multiple gradual fault modes.

FMPF process	FMPF based expectation estimation matrices	Number of used historical statistics
FMPF-1	$\boldsymbol{A}+\Delta\boldsymbol{A}_{\rm E}=\begin{bmatrix}0 & 1 & 0 & 0\\ 0 & -31.4084 & 2.0704\times10^{-6} & 0\\ 0 & -3.20\times10^{10} & -5.9864\times10^{2} & 5.8776\times10^{13}\\ 0 & 0 & 0 & -1.0\times10^{2}\end{bmatrix}, \boldsymbol{B}+\Delta\boldsymbol{B}_{\rm E}=\begin{bmatrix}0\\0\\0\\0.3040\end{bmatrix}$	30 periods
FMPF-2	$\boldsymbol{A}+\Delta\boldsymbol{A}_{\rm E}=\begin{bmatrix}0 & 1 & 0 & 0\\ 0 & -59.5775 & 2.0704\times10^{-6} & 0\\ 0 & -0.64\times10^{11} & -1.6326\times10^{2} & 1.1755\times10^{13}\\ 0 & 0 & 0 & -0.5\times10^{2}\end{bmatrix}, \boldsymbol{B}+\Delta\boldsymbol{B}_{\rm E}=\begin{bmatrix}0\\0\\0\\0.1216\end{bmatrix}$	25 periods
FMPF-3	$\boldsymbol{A}+\Delta\boldsymbol{A}_{\rm E}=\begin{bmatrix}0 & 1 & 0 & 0\\ 0 & -87.7465 & 2.0704\times10^{-6} & 0\\ 0 & -0.480\times10^{11} & -1.5510\times10^{2} & 0.8816\times10^{13}\\ 0 & 0 & 0 & -0.25\times10^{2}\end{bmatrix}, \boldsymbol{B}+\Delta\boldsymbol{B}_{\rm E}=\begin{bmatrix}0\\0\\0\\0.0532\end{bmatrix}$	20 periods
FMPF-4	$\boldsymbol{A}+\Delta\boldsymbol{A}_{\rm E}=\begin{bmatrix}0 & 1 & 0 & 0\\ 0 & -115.9155 & 2.0704\times10^{-6} & 0\\ 0 & -0.32\times10^{11} & -1.2517\times10^{2} & 0.5877\times10^{13}\\ 0 & 0 & 0 & -0.1667\times10^{2}\end{bmatrix}, \boldsymbol{B}+\Delta\boldsymbol{B}_{\rm E}=\begin{bmatrix}0\\0\\0\\0.0304\end{bmatrix}$	15 periods
FMPF-5	$\boldsymbol{A}+\Delta\boldsymbol{A}_{\rm E}=\begin{bmatrix}0 & 1 & 0 & 0\\ 0 & -144.0845 & 2.0704\times10^{-6} & 0\\ 0 & -0.16\times10^{11} & -0.6259\times10^{2} & 0.2939\times10^{13}\\ 0 & 0 & 0 & -0.125\times10^{2}\end{bmatrix}, \boldsymbol{B}+\Delta\boldsymbol{B}_{\rm E}=\begin{bmatrix}0\\0\\0\\0.0190\end{bmatrix}$	10 periods

5.2. Simulation results with FTC strategies

The first case (Fig. 5) represents system response of an actuation system experiencing gradual faults to a step input with the displacement of 0.03 m. Two methods, based on the FTC approaches, are used to compare the system response. The first is FTC approach presented in Ref. [29], which models the effects of gradual faults as system uncertain modes and applies robust control method to obtain the control parameters. The second is the FMPF based FTC approach. The method first estimates the unknown parameters using FMPF method on the historical statistics of the system experiencing gradual faults, and then determines the control parameters based on the estimated system. The simulation results indicate that system with FMPF based FTC approach has improved tracking performance (Fig. 5(a)). The results (Fig. 5(b)) also indicate that using FMPF based FTC approach results in smaller tracking error.

The same FTC approaches as the ones used in Fig. 5 are used to compare the control effects when the sinusoidal input signal is applied to the actuation system experiencing gradual

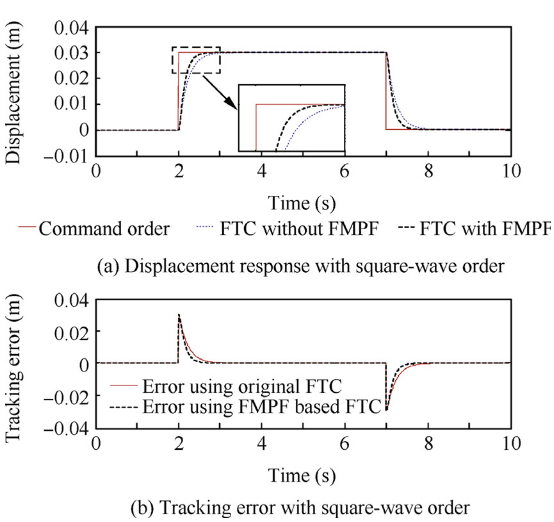

(a) Displacement response with square-wave order

(b) Tracking error with square-wave order

Fig. 5 Tracking response using original FTC and proposed FMPF based FTC when given square-wave order.

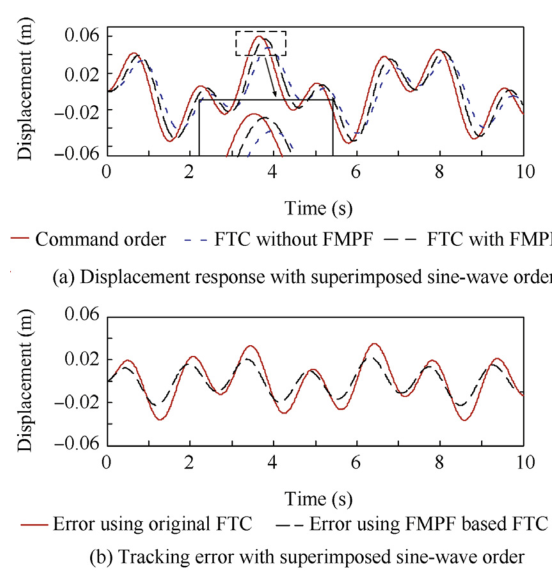

(a) Displacement response with superimposed sine-wave order

(b) Tracking error with superimposed sine-wave order

Fig. 6 Tracking response using original FTC and proposed FMPF based FTC when given superimposed sine-wave order.

faults. The simulation results are shown in Fig. 6, which indicate that the proposed controller has good tracking performance. Specifically, Fig. 6(a) indicates that using FMPF based FTC approach results in close tracking of the input signal, where the amplitudes of the system response are very close to the ones of the given command, and the response time delay is also smaller than using the FTC approach without FMPF. Also, Fig. 6(b) indicates that FMPF based FTC approach results in the system having smaller tracking error under the given command.

The effects of the historical statistics are analyzed by managing different amount of historical statistic using the proposed FMPF approach. Using the proposed FMPF method, five different models are designated as FMPF-1 – 5, where the model based on FMPF-1 is obtained based on the largest amount of historical statistic, whereas the FMPF-5 induced model is obtained using the least amount of historical statistic.

The simulation results, for the case when a step signal with displacement of 0.03[m] is given as the command input to the actuation system experiencing gradual faults, are shown in Fig. 6. Using the same proposed FMPF based FTC approach, five models, based on different amount of historical statistic, are used to compare the control effects on system response. Fig. 7(a) shows that system response has the settling rise time under the FMPF-1 based FTC approach, whereas FMPF-5 based FTC approach results in the slowest settling time. The results presented in Fig. 7(b) indicate that FMPF-1 based FTC approach results in the lowest tracking error for the given command, whereas FMPF-5 based FTC approach results in the highest tracking error. Since FMPF-1 manages the largest amount of historical statistic and FMPF-5 manages the least amount of historical statistic, it illustrates that, within the coverage of MW size, more historical statistic used results in better control performance.

The simulation results presented in Fig. 8 are for the case when a sinusoidal signal is the command input to the actuation system experiencing gradual faults. The same FTC approach, i.e. five models based on different amount of historical statistic, is used to compare the control effects. The results presented in Fig. 8(a) indicate that FMPF-1 based FTC approach results in the best tracking performance, whereas FMPF-5 based FTC approach results in the worst tracking performance. The simulation results presented in Fig. 8(b) show that FMPF-1 based FTC approach results in the minimum tracking error, while FMPF-5 based FTC approach results in the maximum tracking error. It is apparent that, within the coverage of MW size, using more historical statistic results in better control performance.

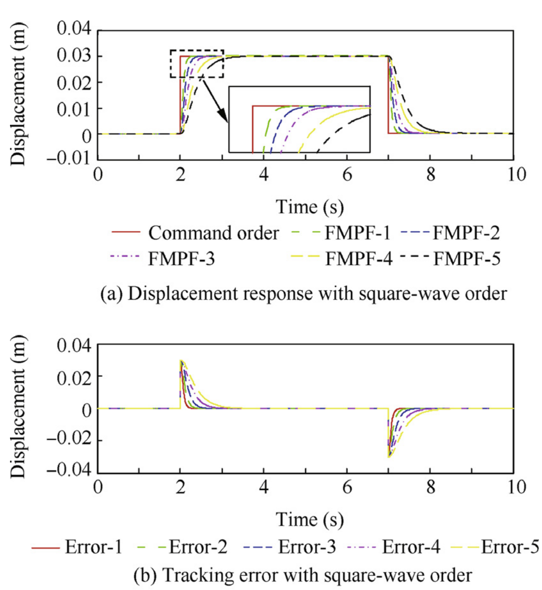

Fig. 7 Tracking responses of when given square-wave order using different FMPF based FTC.

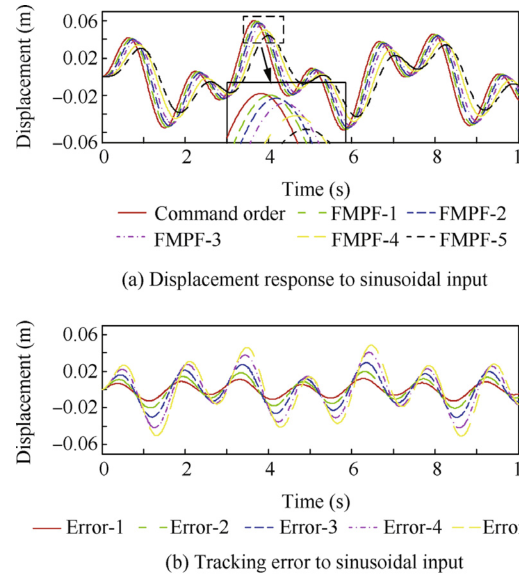

Fig. 8 Tracking responses when given superimposed sine-wave order using different FMPF based FTC.

6. Conclusions

A Fault Mode Probability Factor (FMPF)-based Fault-Tolerant Control (FTC) strategy for multiple gradual faults of Dissimilar Redundant Actuation System (DRAS) has been studied and evaluated. The typical gradual faults of DRAS system are modeled into the state space system in uncertainty form. The historical statistics of the fault modes are used to modify and correct the uncertain model using the proposed FMPF. A controller with fixed structure in state and output error integration feedback form is designed based on the modified model using FMPF. New updating method for the initial control gain under gradual fault condition is proposed. The simulation results indicate that the proposed FMPF based FTC control strategy is effective for the long term working condition of DRAS system experiencing gradual faults. The proposed strategy indicates that system response improves by increasing the amount of historical statistics.

In order to develop the strategy for a wider range of applications, the future work will address optimization of the MW size as well as applicability of the proposed FMPF based FTC strategy on the nonlinear systems.

Acknowledgements

This work was co-supported by the National Natural Science Foundation of China (Nos. 51620105010, 51675019 and

51575019), the National Basic Research Program of China (No. 2014CB046402), the Fundamental Research Funds for the Central Universities of China (YWF-17-BJ-Y-105) and the "111" Project of China.

Appendix A. Proof of Lemma 1

Proof. The eigenvalue form of the uncertain system model, to transform the pair matrix $(\boldsymbol{A}+\Delta\boldsymbol{A},\boldsymbol{B}+\Delta\boldsymbol{B})$ with $\boldsymbol{K_x}$, can be obtained as

$$\begin{aligned}&\mathrm{Re}\{\lambda(\boldsymbol{A}+\Delta\boldsymbol{A}+(\boldsymbol{B}+\Delta\boldsymbol{B})\boldsymbol{K_x})\}\\&\quad=\mathrm{Re}\{\lambda(\boldsymbol{A})+\rho_{\mathrm{A}}\lambda(|\Delta\boldsymbol{A}|_{\mathrm{bound}})+\lambda(\boldsymbol{BK_x})\\&\qquad+\rho_{\mathrm{B}}\lambda(|\Delta\boldsymbol{B}|_{\mathrm{bound}}\boldsymbol{K_x})\}\end{aligned}\tag{A1}$$

Let $\rho_{\mathrm{A}}\in[-1,+1]$ and $\rho_{\mathrm{B}}\in[-1,+1]$, express the change of parameters due to gradual faults, and then the following inequality can be obtained:

$$\begin{aligned}&\mathrm{Re}\{\lambda(\boldsymbol{A})+\rho_{\mathrm{A}}\lambda(|\Delta\boldsymbol{A}|_{\mathrm{bound}})+\lambda(\boldsymbol{BK_x})+\rho_{\mathrm{B}}\lambda(|\Delta\boldsymbol{B}|_{\mathrm{bound}}\boldsymbol{K_x})\}\\&\quad<-|\mathrm{Re}\{\lambda(\boldsymbol{A})\}|+|\mathrm{Re}\{\lambda(|\Delta\boldsymbol{A}|_{\mathrm{bound}})\}|\\&\qquad-|\mathrm{Re}\{\lambda(\boldsymbol{BK_x})\}|+|\mathrm{Re}\{\lambda(|\Delta\boldsymbol{B}|_{\mathrm{bound}}\boldsymbol{K_x})\}|\end{aligned}\tag{A2}$$

From Eq. (A2), it can be deduced that

$$\begin{aligned}&\mathrm{Re}\{\lambda(\boldsymbol{A}+\Delta\boldsymbol{A}+(\boldsymbol{B}+\Delta\boldsymbol{B})\boldsymbol{K_x})\}\\&\quad<\max(\mathrm{Re}\{\lambda(\boldsymbol{A})\pm\lambda(|\Delta\boldsymbol{A}|_{\mathrm{bound}})+\lambda(\boldsymbol{BK_x})\\&\qquad\pm\lambda(|\Delta\boldsymbol{B}|_{\mathrm{bound}}\boldsymbol{K_x})\})\end{aligned}\tag{A3}$$

The real parts of eigenvalues for the FMPF based amended model can be expressed as

$$\begin{aligned}&\mathrm{Re}\left\{\lambda\left(\boldsymbol{A}+\left(\sum_{j=1}^{k}(P_{c_j}(\Delta\boldsymbol{A}_{T_i}))\right)+\left(\boldsymbol{B}+(\sum_{j=1}^{k}(P_{c_j}(\Delta\boldsymbol{B}_{T_i})))\right)\boldsymbol{K_x}\right)\right\}\\&=\mathrm{Re}\left\{\lambda(\boldsymbol{A})+\lambda\left(\sum_{j=1}^{k}(P_{c_j}(\Delta\boldsymbol{A}_{T_i}))\right)+\lambda(\boldsymbol{BK_x})+\lambda\left(\left(\sum_{j=1}^{k}(P_{c_j}(\Delta\boldsymbol{B}_{T_i}))\right)\boldsymbol{K_x}\right)\right\}\\&=\mathrm{Re}\{\lambda(\boldsymbol{A})+\lambda(\boldsymbol{A}_{\mathrm{E}})+\lambda(\boldsymbol{BK_x})+\lambda(\boldsymbol{B}_{\mathrm{E}}\boldsymbol{K_x})\}\end{aligned}\tag{A4}$$

The real parts of eigenvalues for the actual model can be expressed as

$$\begin{aligned}&\mathrm{Re}\{\lambda(\boldsymbol{A}+\boldsymbol{A}_{\mathrm{actual}}+(\boldsymbol{B}+\boldsymbol{B}_{\mathrm{actual}})\boldsymbol{K_x})\}\\&\quad=\mathrm{Re}\{\lambda(\boldsymbol{A})+\boldsymbol{\lambda}(\boldsymbol{A}_{\mathrm{actual}})+\lambda(\boldsymbol{BK_x})+\lambda(\boldsymbol{B}_{\mathrm{actual}}\boldsymbol{K_x})\}\end{aligned}\tag{A5}$$

Then two errors can be obtained: One is the error between the real parts of eigenvalues for the FMPF based amended model and the actual one, whereas the other is the error between the real parts of eigenvalues for the uncertain model and the actual one. In order to prove the advantage of FMPF based FTC approach, it needs to be shown that the absolute value of the first error is less than the second one.

The error between the real parts of eigenvalues for the FMPF based amended model and the actual one can be determined as follows:

$$\begin{aligned}&\mathrm{Re}\left\{\lambda\left(\boldsymbol{A}+\left(\sum_{j=1}^{k}(P_{c_j}(\Delta\boldsymbol{A}_{T_i}))\right)+\left(\boldsymbol{B}+\left(\sum_{j=1}^{k}(P_{c_j}(\Delta\boldsymbol{B}_{T_i}))\right)\right)\boldsymbol{K_x}\right)\right\}\\&-\mathrm{Re}\{\lambda(\boldsymbol{A}+\boldsymbol{A}_{\mathrm{actual}}+(\boldsymbol{B}+\boldsymbol{B}_{\mathrm{actual}})\boldsymbol{K_x})\}\\&=\mathrm{Re}\{\lambda(\boldsymbol{A})+\lambda(\boldsymbol{A}_{\mathrm{E}})+\lambda(\boldsymbol{BK_x})+\lambda(\boldsymbol{B}_{\mathrm{E}}\boldsymbol{K_x})\}\\&\quad-\mathrm{Re}\{\lambda(\boldsymbol{A})+\lambda(\boldsymbol{A}_{\mathrm{actual}})+\lambda(\boldsymbol{BK_x})+\lambda(\boldsymbol{B}_{\mathrm{actual}}\boldsymbol{K_x})\}\\&=\mathrm{Re}\{\lambda(\boldsymbol{A}_{\mathrm{E}})-\lambda(\boldsymbol{A}_{\mathrm{actual}})+\lambda(\boldsymbol{B}_{\mathrm{E}}\boldsymbol{K_x})-\lambda(\boldsymbol{B}_{\mathrm{actual}}\boldsymbol{K_x})\}\end{aligned}\tag{A6}$$

Define the absolute value of this error as

$$\mathrm{Error}(M_1)=|\mathrm{Re}\{\lambda(\boldsymbol{A}_{\mathrm{E}})-\lambda(\boldsymbol{A}_{\mathrm{actual}})+\lambda(\boldsymbol{B}_{\mathrm{E}}\boldsymbol{K_x})-\lambda(\boldsymbol{B}_{\mathrm{actual}}\boldsymbol{K_x})\}|\tag{A7}$$

The error between the real parts of eigenvalues for the uncertain model and the actual one can be calculated as

$$\begin{aligned}&\mathrm{Re}\{\lambda(\boldsymbol{A}+\Delta\boldsymbol{A}+(\boldsymbol{B}+\Delta\boldsymbol{B})\boldsymbol{K_x})\}\\&-\mathrm{Re}\{\lambda(\boldsymbol{A}+\boldsymbol{A}_{\mathrm{actual}}+(\boldsymbol{B}+\boldsymbol{B}_{\mathrm{actual}})\boldsymbol{K_x})\}\\&\quad=\mathrm{Re}\{\lambda(\boldsymbol{A})+\rho_{\mathrm{A}}\lambda(|\Delta\boldsymbol{A}|_{\mathrm{bound}})+\lambda(\boldsymbol{BK_x})\\&\qquad+\rho_{\mathrm{B}}\lambda(|\Delta\boldsymbol{B}|_{\mathrm{bound}}\boldsymbol{K_x})\}-\mathrm{Re}\{\lambda(\boldsymbol{A})+\boldsymbol{\lambda}(\boldsymbol{A}_{\mathrm{actual}})\\&\qquad+\lambda(\boldsymbol{BK_x})+\lambda(\boldsymbol{B}_{\mathrm{actual}}\boldsymbol{K_x})\}=\mathrm{Re}\{\rho_{\mathrm{A}}\lambda(|\Delta\boldsymbol{A}|_{\mathrm{bound}})\\&\qquad-\lambda(\boldsymbol{A}_{\mathrm{actual}})+\rho_{\mathrm{B}}\lambda(|\Delta\boldsymbol{B}|_{\mathrm{bound}}\boldsymbol{K_x})-\lambda(\boldsymbol{B}_{\mathrm{actual}}\boldsymbol{K_x})\}\end{aligned}\tag{A8}$$

Define the absolute value of this error as

$$\begin{aligned}\mathrm{Error}(M_2)=&|\mathrm{Re}\{\rho_{\mathrm{A}}\lambda(|\Delta\boldsymbol{A}|_{\mathrm{bound}})-\lambda(\boldsymbol{A}_{\mathrm{actual}})\\&+\rho_{\mathrm{B}}\lambda(|\Delta\boldsymbol{B}|_{\mathrm{bound}}\boldsymbol{K_x})-\lambda(\boldsymbol{B}_{\mathrm{actual}}\boldsymbol{K_x})\}|\end{aligned}\tag{A9}$$

Since the minimum of the error is the following form:

$$\begin{aligned}\min(\mathrm{Error}(M_2))=&|\mathrm{Re}\{\lambda(|\Delta\boldsymbol{A}|_{\mathrm{bound}})-\lambda(\boldsymbol{A}_{\mathrm{actual}})\\&+\lambda(|\Delta\boldsymbol{B}|_{\mathrm{bound}}\boldsymbol{K_x})-\lambda(\boldsymbol{B}_{\mathrm{actual}}\boldsymbol{K_x})\}|\end{aligned}\tag{A10}$$

therefore, $\mathrm{Error}(M_1)-\min(\mathrm{Error}(M_2))=\mathrm{Re}\{\lambda(\boldsymbol{A}_{\mathrm{E}})-\lambda(|\Delta\boldsymbol{A}|_{\mathrm{bound}})+\lambda(\boldsymbol{B}_{\mathrm{E}}\boldsymbol{K_x})-\lambda(|\Delta\boldsymbol{B}|_{\mathrm{bound}}\boldsymbol{K_x})\}$,where due to the expectation theory, at least the following conclusion can hold:

$$\begin{cases}\mathrm{Re}\{\lambda(\boldsymbol{A}_{\mathrm{E}})\}<\mathrm{Re}\{\lambda(|\Delta\boldsymbol{A}|_{\mathrm{bound}})\}\\\mathrm{Re}\{\lambda(\boldsymbol{B}_{\mathrm{E}}\boldsymbol{K_x})\}<\mathrm{Re}\{\lambda(|\Delta\boldsymbol{B}|_{\mathrm{bound}}\boldsymbol{K_x})\}\end{cases}\tag{A11}$$

Eq. (A11) deduces the conclusion that $\mathrm{Error}(M_1)<\min(\mathrm{Error}(M_2))$, so that

$$\mathrm{Error}(M_1)<\mathrm{Error}(M_2)\tag{A12}$$

This proves Lemma 1.

Appendix B. Proof of Theorem 1

Proof. Since the control law form $\boldsymbol{u}(t)=\boldsymbol{Kx}_{\mathrm{aug}}(t)=\boldsymbol{K_e}\int_0^t\boldsymbol{e}(\tau)\mathrm{d}\tau+\boldsymbol{K_x x}(t)$ is used to stabilize the augmented system given in Eq. (12), using the method similar with the one used in Ref.[26], this control law form is substituted into the LQ cost function form

$$
\begin{aligned}
\boldsymbol{J} &= \int_0^t \boldsymbol{x}_{\mathrm{aug}}^{\mathrm{T}}(\tau)(\boldsymbol{Q}+\boldsymbol{K}^{\mathrm{T}}\boldsymbol{R}\boldsymbol{K})\boldsymbol{x}_{\mathrm{aug}}(\tau)\mathrm{d}\tau \\
&< -\int_0^t \boldsymbol{x}_{\mathrm{aug}}^{\mathrm{T}}(\tau)[(\boldsymbol{A}_{\mathrm{aug}}+\boldsymbol{B}_{\mathrm{aug}}\boldsymbol{K})^{\mathrm{T}}\boldsymbol{P}+\boldsymbol{P}(\boldsymbol{A}_{\mathrm{aug}}+\boldsymbol{B}_{\mathrm{aug}}\boldsymbol{K}) \\
&\qquad +\left(\frac{1}{\gamma^2}\right)\boldsymbol{P}\boldsymbol{G}_{\mathrm{aug}}\boldsymbol{G}_{\mathrm{aug}}^{\mathrm{T}}\boldsymbol{P}]\boldsymbol{x}_{\mathrm{aug}}(\tau)\mathrm{d}\tau \\
&= -\int_0^t [(\dot{\boldsymbol{x}}_{\mathrm{aug}}(\tau)-\boldsymbol{G}_{\mathrm{aug}}\boldsymbol{w}_{\mathrm{aug}}(\tau))^{\mathrm{T}}\boldsymbol{P}\boldsymbol{x}_{\mathrm{aug}}(\tau)+\boldsymbol{x}_{\mathrm{aug}}^{\mathrm{T}}(\tau)\boldsymbol{P}(\dot{\boldsymbol{x}}_{\mathrm{aug}}(\tau) \\
&\qquad -\boldsymbol{G}_{\mathrm{aug}}\boldsymbol{w}_{\mathrm{aug}}(\tau))+\boldsymbol{x}_{\mathrm{aug}}^{\mathrm{T}}(\tau)\left(\frac{1}{\gamma^2}\right)\boldsymbol{P}\boldsymbol{G}_{\mathrm{aug}}\boldsymbol{G}_{\mathrm{aug}}^{\mathrm{T}}\boldsymbol{P}\boldsymbol{x}_{\mathrm{aug}}(\tau)]\mathrm{d}\tau \\
&\leqslant -\int_0^t \mathrm{d}(\boldsymbol{x}_{\mathrm{aug}}^{\mathrm{T}}(\tau)\boldsymbol{P}\boldsymbol{x}_{\mathrm{aug}}(\tau))+\gamma^2\int_0^t \boldsymbol{w}_{\mathrm{aug}}^{\mathrm{T}}(\tau)\boldsymbol{w}_{\mathrm{aug}}(\tau)\mathrm{d}\tau \\
&= \boldsymbol{x}_{\mathrm{aug}}^{\mathrm{T}}(0)\boldsymbol{P}\boldsymbol{x}_{\mathrm{aug}}(0)+\gamma^2\int_0^t \boldsymbol{w}_{\mathrm{aug}}^{T}(\tau)\boldsymbol{w}_{\mathrm{aug}}(\tau)\mathrm{d}\tau
\end{aligned}
\tag{B1}
$$

This proves Theorem 1.

References

1. Wang JS, Li ZY, Peng B. Modeling and analysis of the dissimilar redundant actuator system. *Mach Tool Hydraul* 2008;**36**(6):79–81.
2. Wang SP, Cui XY, Shi J, Tomovic MM, Jiao ZX. Modeling of reliability and performance assessment of a dissimilar redundancy actuation system with failure monitoring. *Chin J Aeronautics* 2016;**29**(3):799–813.
3. Fu YL, Pang YL, He S, Wang LJ. Design and working mode analysis of dissimilar redundant actuator system. *J Beijing Univ Aeronautics Astronautics* 2012;**38**(4):432–7 [Chinese].
4. Wang J, Wang SP, Wang XJ, Shi C, Tomovic MM. Active fault tolerant control for vertical tail damaged aircraft with dissimilar redundant actuation system. *Chin J Aeronaut* 2016;**29**(5):1313–25.
5. Van Den Bossche D. The A380 flight control electrohydrostatic actuators, achievements and lessons learnt. *25th international congress of the aeronautical sciences*. 2006.p. 1–8.
6. Jiang J, Yu X. Fault-tolerant control systems: a comparative study between active and passive approaches. *Annu Rev Control* 2012;**36**(1):60–72.
7. Patton RJ. Fault-tolerant control: The 1997 situation. *IFAC Proceedings Volumes* 1997;**30**(18):1029–51.
8. Zhang Y, Jiang J. Bibliographical review on reconfigurable fault-tolerant control systems. *Annu Rev Control* 2008;**32**(2):229–52.
9. Oberkampf WL, Helton JC, Joslyn CA, Wojtkiewicz SF, Ferson S. Challenge problems: uncertainty in system response given uncertain parameters. *Reliab Eng Syst Saf* 2004;**85**(1):11–9.
10. Ljung L. *Signal analysis and prediction*. Boston, MA: Birkhäuser; 1998. p. 163–73.
11. Goodwin GC, Payne RL. *Dynamic system identification: Experiment design and data analysis*. New York: Springer Science & Business Media; 1977. p. 82–120.
12. Chen S, Billings SA, Luo W. Orthogonal least squares methods and their application to non-linear system identification. *International Journal of Control* 1989;**50**(5):1873–96.
13. Chen T, Andersen MS, Ljung L, Chiuso A, Pillonetto G. System identification via sparse multiple kernel-based regularization using sequential convex optimization techniques. *IEEE Trans Automatic Control* 2014;**59**(11):2933–45.
14. Dullerud GE, Paganini F. *A course in robust control theory: A convex approach*. New York: Springer Science & Business Media; 2013. p. 270–95.
15. Campos VA, Cruz JJ, Zanetta LC. Robust control of dynamical systems using linear matrix inequalities and norm-bounded uncertainty. *J Control, Automation Electr Syst* 2014;**2**(25):151–60.
16. Chang M. *Adaptive design theory and implementation using sas and r*. Abingdon: CRC Press; 2014. p. 51–68.
17. Åström KJ, Wittenmark B. *Adaptive control*. New York: Springer Science & Business Media; 2013. p. 348–70.
18. Chen J, Zhang W, Cao Y-Y. Robust reliable feedback controller design against actuator faults for linear parameter-varying systems in finite-frequency domain. *IET Control Theory Appl* 2015;**9**(10):1595–607.
19. Bemporad A, Morari M, Dua V, Pistikopoulos EN. The explicit linear quadratic regulator for constrained systems. *Automatica* 2002;**38**(1):3–20.
20. Zhang H, Shi Y, Mu B. Optimal h∞-based linear-quadratic regulator tracking control for discrete-time takagi–sugeno fuzzy systems with preview actions. *J Dyn Syst Measure Control* 2013;**135**(4):044501.
21. Palanisamy M, Modares H, Lewis FL, Aurangzeb M. Continuous-time q-learning for infinite-horizon discounted cost linear quadratic regulator problems. *IEEE Trans Cybernetics* 2015;**45**(2):165–76.
22. Shi C, Wang XJ, Wang SP, Wang J, Tomovic MM. Adaptive decoupling synchronous control of dissimilar redundant actuation system for large civil aircraft. *Aerospace Sci Technol* 2015;**47**:114–24.
23. Shi C, Wang SP, Wang XJ, Wang J, Tomovic MM. Active fault-tolerant control of dissimilar redundant actuation system based on performance degradation reference models. *J Franklin Inst* 2017;**354**(2):1087–108.
24. Zhao X, Zhang S, Zhou C, Hu Z, Li R, Jiang J. Experimental study of hydraulic cylinder leakage and fault feature extraction based on wavelet packet analysis. *Comput Fluids* 2015;**106**:33–40.
25. Sepehri LAN. Hydraulic actuator leakage fault detection using extended Kalman filter. *Int J Fluid Power* 2005;**6**:41–5.
26. Chesi G. Lmi conditions for time-varying uncertain systems can be non-conservative. *Automatica* 2011;**47**(3):621–4.
27. Liao F, Wang JL, Yang G-H. Reliable robust flight tracking control: An lmi approach. *IEEE Trans Control Syst Technol* 2002;**10**(1):76–89.
28. Xiang Y, Youmin Z. Design of passive fault-tolerant flight controller against actuator failures. *Chin J Aeronautics* 2015;**28**(1):180–90.
29. Li X, Liu HH. A passive fault tolerant flight control for maximum allowable vertical tail damaged aircraft. *J Dyn Syst Measure Control* 2012;**134**(3):031006.